Experimental investigation of the effect of the intake air temperature and mixture quality on the combustion of a methanol- and gasoline-fuelled homogeneous charge compression igni...

2 authors, including:

Avinash Kumar Agarwal
Indian Institute of Technology Kanpur
580 PUBLICATIONS   **23,048** CITATIONS

SEE PROFILE

Experimental investigation of the effect of the intake air temperature and mixture quality on the combustion of a methanol- and gasoline-fuelled homogeneous charge compression ignition engine

R K Maurya and **A K Agarwal**[*]
Engine Research Laboratory, Department of Mechanical Engineering, Indian Institute of Technology Kanpur, Kanpur, India

Abstract: Environmental concerns have increased significantly all over the world in the past decade. To fulfil the simultaneous emission requirements for near-zero pollutant and low carbon dioxide (CO_2) levels, which are the challenges for the future powertrains, many studies are currently being carried out on new engine combustion processes, such as controlled autoignition for gasoline engines and homogeneous charge compression ignition (HCCI) for diesel engines. These combustion processes have the potential for ultra-low nitrogen oxide (NO_x) and particulate matter emissions in comparison with conventional gasoline or diesel engines.

In this paper, the combustion characteristics of a HCCI engine fuelled with methanol and gasoline were investigated on a modified two-cylinder four-stroke engine. The port fuel injection technique is used to prepare a homogeneous charge of fuel and air. The experiment is conducted with various intake air temperatures ranging from 120 °C to 160 °C at different air-to-fuel ratios, for which stable HCCI combustion is achieved. The experimental results indicate that the inlet air temperature and air-to-fuel ratio have a significant effect on the maximum in-cylinder pressure and its position relative to top dead centre, the shape of the pressure rise curve, and the heat release rates. The results confirm that the inlet air temperature is a very sensitive parameter in controlling combustion timing and thus the effectiveness of the HCCI combustion process.

Keywords: controlled autoignition, homogeneous charge compression ignition, methanol, gasoline, combustion

1 INTRODUCTION

Emissions legislations for new automotive engines are becoming ever more stringent worldwide. A promising technology for considerably reducing the pollutants and fuel consumption of an internal combustion engine is homogeneous charge compression ignition (HCCI) technology. A HCCI engine is an autoignition engine, in which a homogeneous mixture of air and fuel is supplied to the combustion chamber and is made to autoignite (detonate) by compression alone using the movement of the piston. Since low-temperature combustion is realized using super lean mixtures, which are beyond the flammability limits, this homogeneous combustion leads to extremely low emissions and very high combustion efficiencies.

HCCI combustion is achieved by controlling the temperature, pressure, and composition of the air–fuel mixture so that ignition occurs spontaneously in the engine. Thus the required control strategy is significantly more challenging than for a spark ignition (SI) engine or compression ignition (CI) engine

Corresponding author: Engine Research Laboratory, Department of Mechanical Engineering, Indian Institute of Technology Kanpur, Kanpur 208016, India.
email: akag@iitk.ac.in

because, in HCCI combustion, the start of combustion (SOC) is a complex function of chemical kinetics and not simply controlled by spark timing as in a SI engine or injection timing as in the case of a CI engine.

HCCI combustion has the potential to have high thermodynamic efficiencies and to produce ultra-low emissions. HCCI engines can have efficiencies as high as CI engines, while producing low nitrogen oxide (NO_x) and particulate matter (PM) emissions [1]. Since HCCI engines can operate on gasoline, diesel, and most alternative fuels, they can be used with current fuel-refining capabilities. In addition, HCCI engines have the potential to be less expensive than CI engines because they could use a lower-pressure fuel injection system and the emission control system would also be less costly and less dependent on scarce precious metals [2].

The earliest experience with HCCI was reported by Onishi *et al.* [3] who described a unique combustion behaviour intermediate between SI and CI. It was called 'active thermo atmosphere combustion (ATAC)'. The HCCI combustion process has been studied successfully in two-stroke engines [3, 4] and four-stroke engines [5–11], and with liquid fuels [3–9] and gaseous fuels [10, 11]. The HCCI family can be distinguished according to the fuel introduction strategy employed [12]. These strategies include port injection [5, 6], early in-cylinder injection [8, 13, 14], late in-cylinder injection [15], and dual-fuel introduction (both in-cylinder and port injection) [12]. The first gasoline-fuelled four-stroke HCCI engine test was published in 1983 by Najt and Foster [5]. Since then, many other HCCI test results have been published using gasoline or other fuels. The early investigations were on the potential of HCCI and its characteristics. In recent years, more emphasis has been placed on controlling the HCCI engine.

Controlling the combustion rate (burn duration) and the SOC is essential in order to use HCCI combustion effectively in real engines. Two distinct control strategies can be used to control the SOC and combustion rate [16]. First, the temperature of the air–fuel mixture can be controlled as the inlet temperature is a sensitive parameter in controlling the HCCI combustion timing [10, 11, 17, 18]. Relatively simple methods use intake air heating or external exhaust gas recirculation (EGR) to heat the air–fuel mixture. More complex methods use a fully variable-valve-timing system to change valve overlap which changes the EGR rate or use a variable-compression-ratio engine to change the peak cylinder pressure and temperature. Second,

changing the autoignition properties of the air–fuel mixture can be utilized. This can be done by fuel blending, or by adjusting the air-to-fuel ratio in conjunction with changing the percentage EGR in the charge. By blending different fuels, the auto-ignition properties of the air–fuel mixtures can be changed to advance or delay the SOC. The air-to-fuel ratio and percentage EGR affects the dilution of the air–fuel charge. By increasing or decreasing the dilution, the SOC is delayed or advanced respectively [19]. In this paper, the inlet air temperature and leaner mixture of air and fuel are used to control the combustion rate and start of ignition.

One of the advantages of HCCI combustion is its intrinsic fuel flexibility. In this paper, experimental investigations of HCCI combustion are carried out on the same HCCI engine using both methanol and gasoline as fuels at different inlet air temperatures. While the use of oxygenated compounds in gasoline started in the 1920s, their use expanded considerably in the 1970s when the rapid increase in crude oil prices made them economically viable. Oxygenated alcohols that are blended in gasoline are methanol, ethanol, isopropanol and *t*-butanol. However, owing to the economics of large-scale production of alcohol fuels, only ethanol and methanol are suitable as stand-alone alternative fuels. The advantages of alcohols are that they can be produced from renewable resources readily available and distributed around the globe. Methanol can be derived from either natural gas or coal and biomass [20]. Methanol can be used as a HCCI engine fuel because methanol exhibits good HCCI combustion characteristics. Methanol has demonstrated a significant widening of the HCCI operating regime compared with gasoline. In experiments performed on a two-stroke SI engine, methanol expanded the air-to-fuel ratio range of operation over that of gasoline and allowed HCCI operation in the idling condition [21].

Gasoline, however, has multiple advantages as a HCCI fuel. Gasoline has a high octane number, which allows the use of reasonably high compression ratios in HCCI engines. Actual compression ratios for gasoline-fuelled HCCI engine varies from 12:1 to 21:1 depending on the fuel octane number, the intake air temperature, and the specific engine used. This compression ratio range allows gasoline-fuelled HCCI engines to achieve relatively high thermal efficiencies. A potential drawback of higher compression ratios is that the engine design must accommodate the relatively high cylinder pressures that are encountered, particularly at high engine loads. Additional advantages of gasoline include easy

evaporation, simpler mixture preparation, and a ubiquitous refuelling infrastructure [2].

2 EXPERIMENTAL DETAILS

A two-cylinder four-stroke air-cooled, naturally aspirated direct-injection diesel engine with a bowl-shaped combustion chamber was modified for the present experiment. The specifications of the unmodified engine are given in Table 1. One of the two cylinders of the engine is modified to operate in HCCI mode, while the other cylinder operated like a conventional diesel engine, thus motoring the first cylinder for achieving HCCI combustion. A schematic diagram of the experimental set-up is shown in Fig. 1.

Table 1 Detailed engine specifications

Engine characteristics	Specifications
Model	Indec PH2 diesel engine
Injection type	Direct injection
Number of cylinders	Two
Bore	87.3 mm
Stroke	110 mm
Power per cylinder	4.85 kW at 1500 r/min
Compression ratio	16.5
Displacement	1318 cm^3
Fuel injection timing	24° before TDC
Fuel injection pressure	210 kg/cm^2 at 1500 r/min
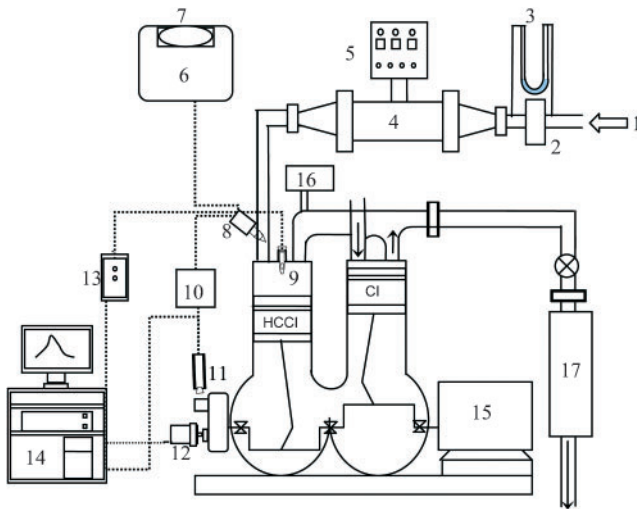
Fig. 1 Schematic diagram of the experimental set-up: 1, intake air; 2, orifice; 3, manometer; 4, heater; 5, heater controller; 6, fuel tank; 7, fuel pump; 8, port fuel injector; 9, pressure transducer; 10, injection timing circuit; 11, TDC sensor; 12, shaft encoder; 13, charge amplifier; 14, data acquisition system; 15, dynamometer; 16, emission analyser; 17, exhaust muffler

The test fuels used for present investigations are methanol and gasoline. A fuel premixing system was installed in the intake manifold. This system consists of an electronic gasoline port injector and an injection start timing (with respect to top dead centre (TDC)) and an injection duration controlling electronic circuit. A controlling circuit developed for this purpose is used to control the pulse width, which in turn triggers the fuel injector. Fresh air entering the engine is heated by an air preheater positioned upstream of the intake manifold. The intake air heater is operated by a closed-loop controller, which maintains a constant intake air temperature as set by the user by feedback control. A thermocouple in conjunction with a digital temperature indicator was used to measure the intake and exhaust gas temperatures. An orifice meter and a U-tube manometer were used to measure the air consumption of the engine. A surge tank fixed on the inlet side of the engine maintains a constant airflow through the orifice meter and dampens cyclic fluctuations.

The in-cylinder pressure was measured using a water-cooled piezoelectric pressure transducer (Kistler; model 6061B) which is mounted flush in the cylinder head. The pressure transducer minimizes thermal shock error by using a double-walled diaphragm and an integral water-cooling system. To measure the crank angle (CA) in degrees, an optical shaft encoder (Encoders India; model ENC58/6-720ABZ/5-24V) is coupled with the crankshaft using a helical coupling. The cylinder pressure history data acquisition and combustion analysis were carried out using a program based on LabVIEW, developed in-house in the Engine Research Laboratory of the Indian Institute of Technology Kanpur.

The in-cylinder pressure was recorded for 100 cycles at a CA resolution of 0.5° and averaged to calculate the indicated mean effective pressure (IMEP), rate of heat release (ROHR), mean gas temperature, and other combustion-related parameters.

2.1 Rate of heat release

The ROHR is calculated from the acquired data using the zero-dimensional heat release model [22]. Consequently, the main combustion parameters were extracted from the heat release and in-cylinder pressure curves. The ROHR was calculated as

$$\frac{dQ(\theta)}{d\theta} = \frac{1}{\gamma-1} V(\theta) \frac{dP(\theta)}{d\theta} + \frac{\gamma}{\gamma-1} P(\theta) \frac{dV(\theta)}{d\theta} \quad (1)$$

The following assumptions were made in this calculation.

1. The cylinder charge was considered to behave as an ideal gas.
2. Distributions of thermodynamic properties inside the combustion chamber were considered to be uniform.
3. Dissociation of combustion products was neglected.
4. No variation in the cylinder mass due to blow-by was considered.
5. Heat transfer from the cylinder is neglected in this model.

2.2 Mean gas temperature

The mean gas temperature is calculated by assuming a uniform temperature within the engine cylinder using ideal gas law [22]. The results are valid between intake valve closing and exhaust valve opening. The mean gas temperature was calculated as

$$T(\theta) = \frac{P(\theta)V(\theta)n(\theta)}{P_{IVC}V_{IVC}n_{IVC}} T_{IVC} \qquad (2)$$

In this calculation, the molar ratio is assumed to be unity.

2.3 Gas exchange efficiency η_{ge}

The gas exchange efficiency is defined as the ratio of the indicated work during the complete cycle to that during the closed part of the cycle [23]. The gas exchange efficiency was calculated as

$$\eta_{ge} = \frac{IMEP_n}{IMEP_g} \qquad (3)$$

2.4 Combustion efficiency

The combustion efficiency was calculated from the equation [24]

$$\eta_{com} = \frac{\sum ROHR}{Q_{in}} \times 100 \qquad (4)$$

where $\Sigma ROHR$ is the integrated value of the heat release rate, and Q_{in} is the total heat value of the introduced fuel.

The cooling losses by convective, radiative, and conductive heat transfer through the wall of combustion chamber were not considered.

2.5 Gross indicated thermal efficiency

The gross indicated thermal efficiency is defined as the ratio of the work $W_{i,g}$ on the piston during the compression and expansion stroke to the input fuel energy [25] according to

$$\eta_{i,g} = \frac{W_{i,g}}{m_f q_{LHV}} \qquad (5)$$

where m_f is the fuel mass per cycle and q_{LHV} is the lower heating value of the fuel.

2.6 Relative air-to-fuel ratio λ

In this work, λ is the ratio of the actual air-to-fuel ratio to the stoichiometric air-to-fuel ratio. The results in this investigation are presented with respect to different relative air–fuel ratios λ, which are present in the HCCI operating region. Experiments were conducted on the modified engine at a constant speed of 1500 r/min and different intake air temperatures.

3 EXPERIMENTAL UNCERTAINTY ANALYSIS

In this paper, the combustion parameters are derived from in-cylinder pressure measurement and analysis. Details of the combustion parameter calculation are given in section 2. To avoid the cyclic variation and uncertainty, the average of 100 pressure cycles is employed to calculate various parameters. The cycle-to-cycle variations in these parameters have been given in reference [26]. Uncertainties in the measurement of different measured quantities are analysed in this section. Table 2 provides the range, accuracy, and percentage uncertainties of various instruments used in this

Table 2 List of instruments and their ranges, accuracies, and uncertainties

Instrument	Range	Accuracy	Percentage uncertainties
Pressure sensor	0–250 bar	± 0.1	± 0.1
TDC sensor		± 1°	± 0.2
Shaft encoder		± 0.5°	± 0.1
Speed-measuring unit	0–1000 r/min	± 10	± 0.1
Manometer		± 1 mm	± 1
Temperature indicator (K-type thermocouple)	0–1000 °C	± 1 °C	± 0.15

experiment for observing various parameters. Errors and uncertainties in the experiments can arise from instrument selection, condition, calibration, environment, observation, reading, and test planning. Uncertainty analysis is needed to prove accuracy in the experiments. An uncertainty analysis was performed using the method described in reference [27]. The percentage uncertainties of parameters such as the air and fuel rates were calculated using the percentage uncertainties of various instruments given in Table 2.

For this experiment,

Total percentage uncertainty

$$
\begin{aligned}
= &\Big[(\text{uncertainty of TDC})^2 + (\text{uncertainty of} \\
&\text{pressure sensor})^2 + (\text{uncertainty of} \\
&\text{temperature indicator})^2 + (\text{uncertainty of air} \\
&\text{flowrate measurement})^2 + (\text{uncertainty} \\
&\text{of fuel flowrate measurement})^2\Big]^{1/2} \\
= &\left(0.2^2 + 0.1^2 + 0.15^2 + 1^2 + 0.2^2\right)^{1/2} \\
= &\pm 1.1\%
\end{aligned} \tag{6}
$$

4 RESULTS AND DISCUSSION

In this section, the experimental results of HCCI combustion of an engine running at different operating conditions at a constant engine speed of 1500 r/min are presented with methanol and gasoline as fuels.

4.1 Operating region

To study the HCCI combustion, criteria as to what constitutes HCCI combustion must be defined. The HCCI operation region is limited by the misfire and the knocking. The operation boundaries are associated with these factors (misfire and knock). The first boundary defines the lower limit for the HCCI combustion. At low loads, the fuel flowrate decreases and hence the net heat release also decreases. It is believed that the resulting gradual reduction in the average combustion temperature results in more unburned charge which is characterized by high carbon monoxide (CO) and total hydrocarbon emissions and by an increase in cycle-to-cycle variation. Cycle-to-cycle variation in the combustion process in an engine can be monitored by the cylinder

pressure transducer. Fluctuation of the IMEP is used as a measure of cycle-to-cycle variations and expressed as COV_{IMEP}. The coefficient of variation (COV) of IMEP was used in this investigation and COV is calculated for 100 consecutive engine cycles as standard deviation σ_{IMEP} divided by the mean value (of IMEP) as a percentage [28] according to

$$
\text{COV}_{\text{IMEP}} = \frac{\sigma_{\text{IMEP}}}{\text{IMEP}} \times 100\% \tag{7}
$$

Since the drivability problems in automobiles normally arise when COV_{IMEP} exceeds 10 per cent [26], this study used this value for defining the misfire boundary.

When the fuelling rate is increased (i.e. lower λ), the HCCI combustion rates also increase, intensify, and gradually cause unacceptable noise (due to severity of detonation); they may potentially cause engine damage and eventually lead to unacceptably high levels of nitrogen oxide (NO_x) emissions. Therefore knocking combustion can be defined as being at the upper limit of HCCI combustion. In this investigation, the upper limit of HCCI combustion is defined as being when the rate of pressure rise in a cylinder exceeds 1.0 MPa CA ($dP/d\theta_{\max} = 1.0$ Mpa/deg CA) for each individual cycle.

The recorded pressure in the cylinder determined the values of both COV_{IMEP} and $dP/d\theta_{\max}$. Therefore, the HCCI operation region is the area in which the value of COV_{IMEP} is less than 10 per cent and value of $dP/d\theta_{\max}$ is less than 1.0 MPa/deg CA. This definition is applied to the present investigation and HCCI operating regions were found for methanol and gasoline (Figs 2 and 3).

It was observed that, for stable HCCI operating conditions, the engine runs at the richest mixture for a lower intake air temperature and, at a higher inlet air temperature, leaner mixtures can be successfully
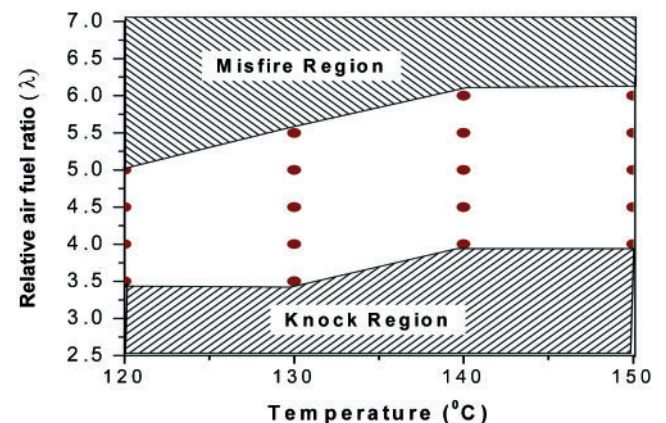

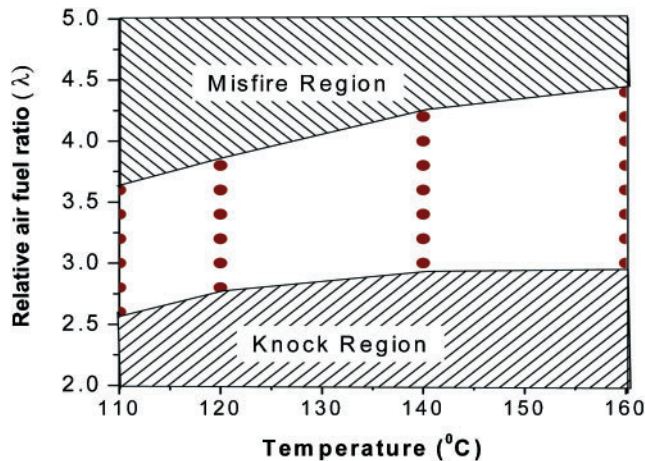**Fig. 2** HCCI stable operating range for methanol

Fig. 3 HCCI stable operating range for gasoline

autoignited. Figures 2 and 3 show that the HCCI operating region was found for methanol in the λ range 3.5–6.5 and for gasoline in the λ range 2.6–4.4 for different intake air temperatures used in the present investigation.

4.2 Cylinder pressure and rate of heat release

The cylinder pressure was measured for all operating conditions and average of 100 cycles with a CA resolution of 0.5° is plotted for HCCI combustion of both fuels (methanol and gasoline). Figures 4 and 5 show the in-cylinder pressure traces and ROHR for methanol and gasoline respectively at different relative air-to-fuel ratios λ and inlet air temperatures. For all plots, the trace with the highest maximum pressure corresponds to the operating condition with the richest mixture, as given by Figs 4 and 5, and the lowest maximum pressure corresponds to the leanest mixture.

On increasing the inlet air temperature at any constant λ, the maximum pressure in the cylinder increases for both fuels (Figs 6(a) and 7(a)). For all plots in Figs 4 and 5, the trace with the highest ROHR corresponds to the operating condition with the richest mixture, and the lowest ROHR corresponds to the leanest mixture at constant inlet air temperature for methanol as well as gasoline. It can also be seen that the SOC is sensitive to the temperature history during the compression stroke, which is dependent on the inlet air temperature.

Figures 6 and 7 show a detailed analysis of combustion parameters and the CA positions of methanol and gasoline respectively. It can be observed from Figs 6(a) and 7(a) that the maximum pressure decreases with increase in λ as less fuel is

available for autoignition and, as a result, it develops a lower maximum pressure. On increasing the inlet air temperature, the maximum pressure increases for both gasoline and methanol at a constant relative air-to-fuel ratio. It can also be seen from the figures that, at constant λ and inlet temperature, the maximum pressure in the cylinder is higher for methanol than for gasoline. Figures 6(c) and 7(c) show the CA positions corresponding to the maximum cylinder pressure for methanol and gasoline respectively. It can be observed that CA position for maximum pressure increases after TDC because the fuel–air mixture becomes leaner. Figures 6(b) and 7(b) show maximum ROHR at different engine operating conditions for methanol and gasoline respectively. It can be noted from these figures that the maximum ROHR is highest corresponding to the richest mixture and lowest for a leaner mixture at constant intake air temperature since less fuel is ignited in the cylinder. Because of advanced ignition timing of the rich fuel–air mixture, the peak values of the ROHR are very high for richer fuel–air mixtures. It can be observed from Figs 6(d) and 7(d) that the CA position corresponding to the maximum ROHR moves away from the TDC as the engine was operated with leaner mixtures at a constant intake air temperature for both gasoline and methanol respectively.

The 10 per cent mass burned fractions (MBFs) of methanol- and gasoline-fuelled engines running in HCCI combustion mode at different engine operating conditions are shown in Figs 6(e) and 7(e) respectively. This can be noted as the SOC in the combustion chamber. It can be seen from the figures that, on increasing the inlet air temperature, the combustion starts earlier at any relative air-to-fuel ratio because the combustion chamber temperature increases. In HCCI combustion, the SOC depends on chemical kinetics, which is dependent on the pressure and temperature history inside the combustion chamber. The variation in the 50% MBF at different engine operating conditions in HCCI mode is shown in Figs 6(f) and 7(f) for methanol and gasoline respectively. It is observed that the 50 per cent MBF has a similar trend to the 10 per cent MBF.

4.3 Engine load (IMEP)

One major limitation of HCCI combustion is the requirement of a highly diluted mixture in order to slow down the speed of the chemical reactions sufficiently, so that the engine is not damaged and this leads to slower combustion. With lean operation,
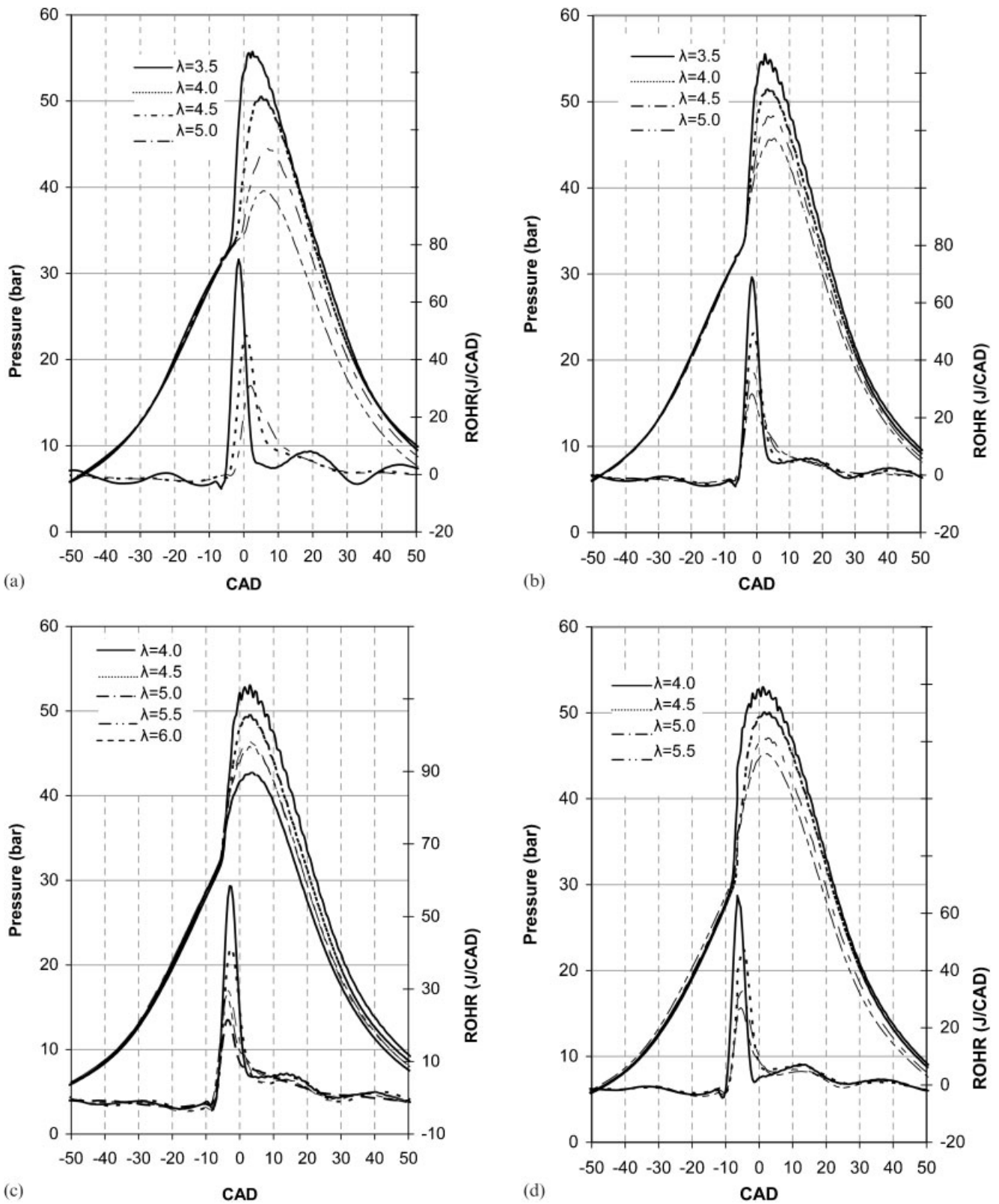
Fig. 4 P–θ and ROHR for different relative air-to-fuel ratios λ at intake air temperatures of (a) 120 °C, (b) 130 °C, (c) 140 °C, and (d) 150 °C for methanol-fuelled HCCI combustion
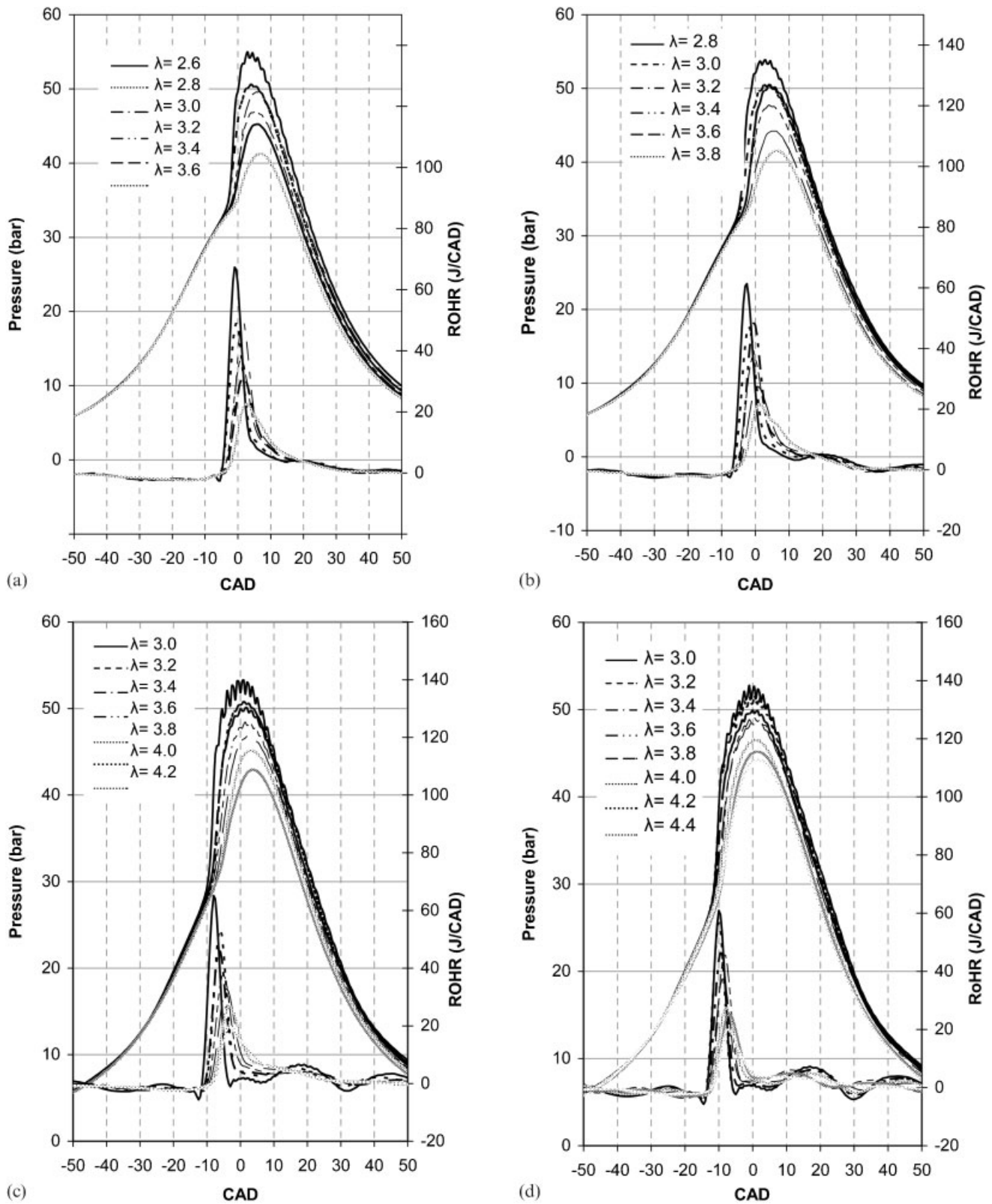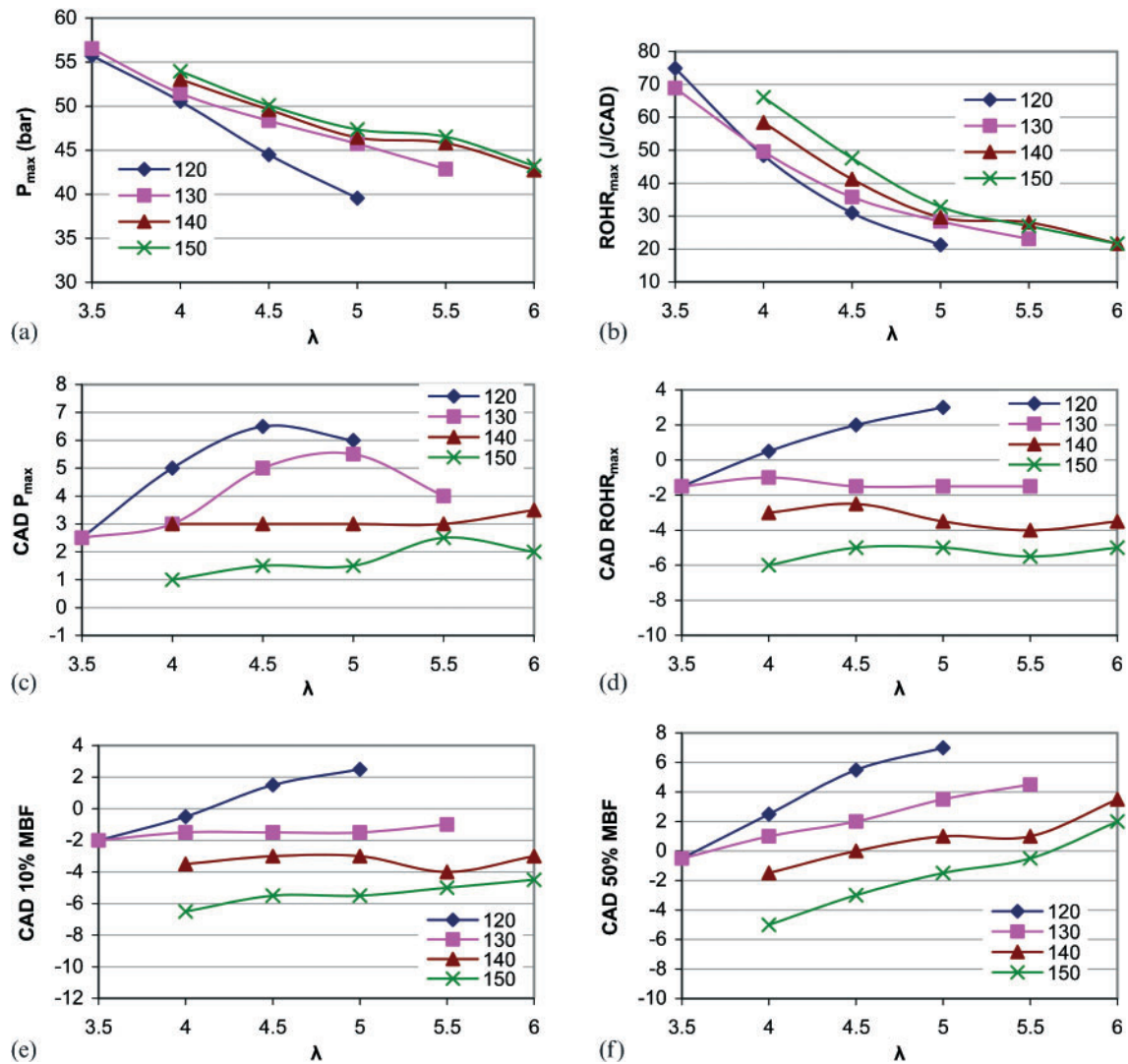
Fig. 5 P–θ and ROHR for different relative air-to-fuel ratios λ at intake air temperatures of (a) 110 °C, (b) 120 °C, (c) 140 °C, and (d) 160 °C for gasoline-fuelled HCCI combustion

Fig. 6 Combustion parameters and CA positions of methanol HCCI combustion at different relative air-to-fuel ratios: (a) maximum cylinder pressure P_{max} (b) $ROHR_{max}$, (c) CA (deg) for P_{max}, (d) CA (deg) for $ROHR_{max}$, (e) CA (deg) for 10 per cent MBF, and (f) CA (deg) for 50 per cent MBF

this will significantly reduce the output for a given airflow through the engine. The rich-side limit for the IMEP is limited by the rate of combustion and hence by the rate of pressure rise. The variation in the IMEP at different engine operating conditions in HCCI mode is shown in Figs 8(a) and 9(a) for methanol and gasoline respectively. The maximum IMEP encountered in this investigation is 3.4 bar for methanol and 3.3 bar for gasoline with operating boundary conditions of COV_{IMEP} and when the maximum rate of pressure rise is less than 10 per cent. It can be noted from these figures that the IMEP decreases as the engine operates with leaner mixtures. This trend for both methanol and gasoline is similar.

It is worth examining the variation in the maximum average gas temperature inside the cylinder since it is directly related to emissions from the engine for HCCI combustion. With homogeneous combustion of a premixed charge, the temperature is expected to be the same throughout the combustion chamber, except near the walls. This, in combination with very lean fuel–air mixtures, gives a low maximum temperature during the cycle. NO_x formation is very sensitive to the peak temperature encountered during combustion. At temperatures above 1800 K, the NO_x formation rate increases rapidly. Figures 8(b) and 9(b) show the variations in the maximum gas temperature at different engine operating conditions for methanol and gasoline fuels
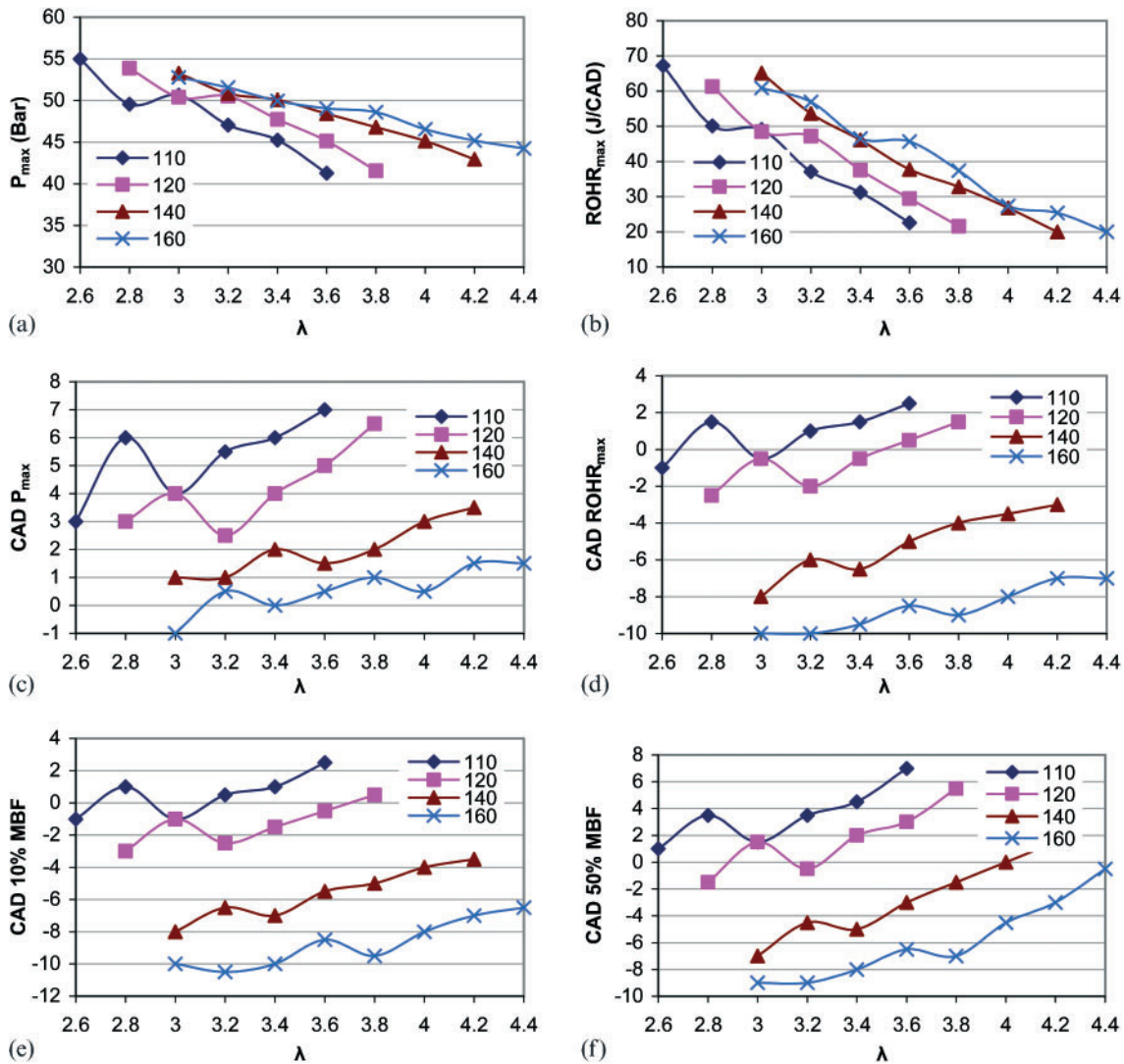
Fig. 7 Combustion parameters and CA positions of gasoline HCCI combustion at different relative air-to-fuel ratios: (a) maximum cylinder pressure P_{max}, (b) $ROHR_{max}$, (c) CA (deg) for P_{max}, (d) CA (deg) for $ROHR_{max}$, (e) CA (deg) for 10 per cent MBF, and (f) CA (deg) for 50 per cent MBF

respectively. It can be seen that the value of the maximum mean gas temperature decreases with increasing λ (i.e. leaner mixtures) at any given intake air temperature and increases with increasing intake air temperature. It can be observed from the figures that the maximum temperature in the combustion chamber is for the richest mixture, which also demonstrated the highest ROHR.
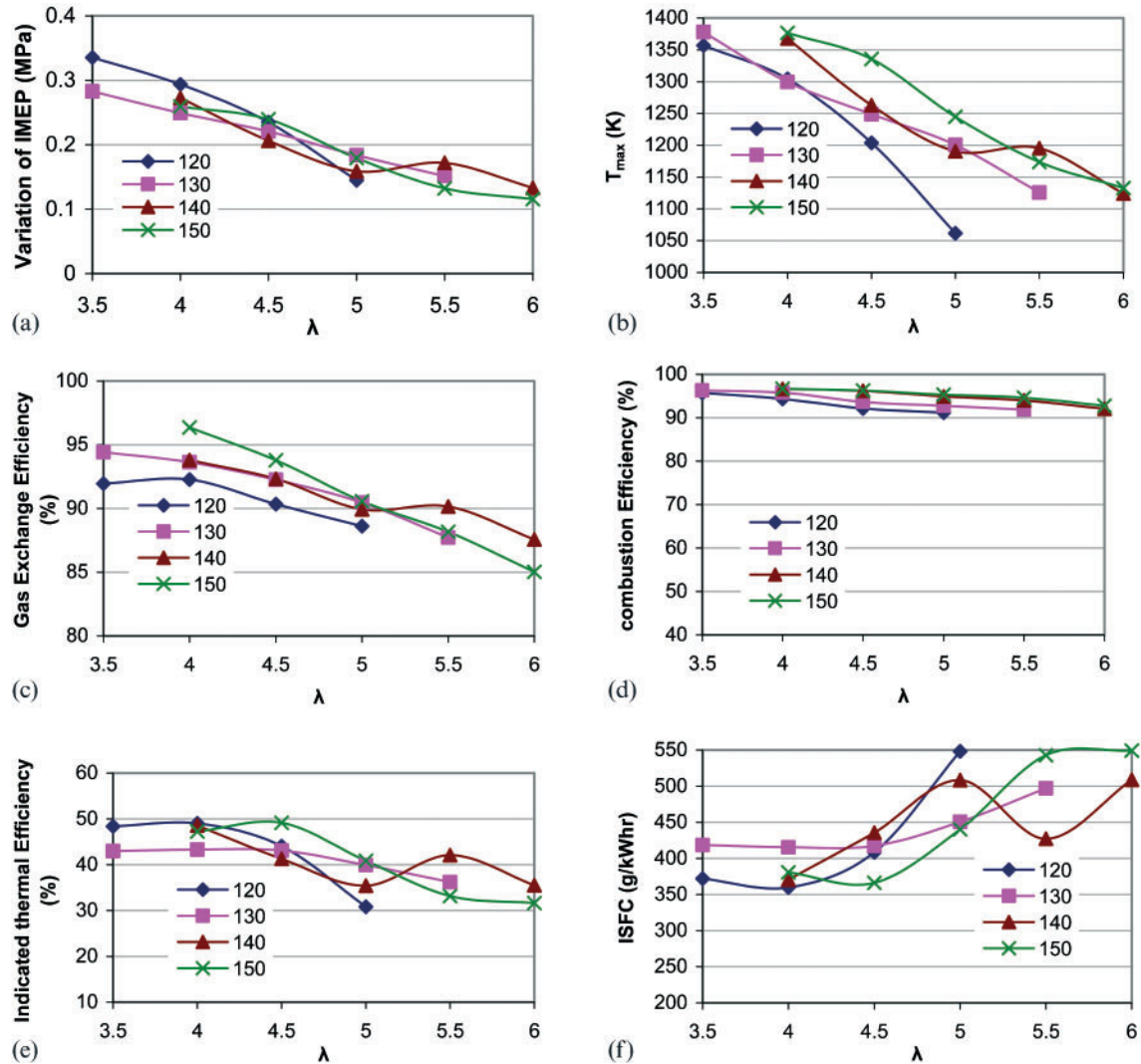
4.4 Gas exchange efficiency

The HCCI engine operates unthrottled, which reduces the pumping losses at part-load compared with the conventional SI engine. The gas exchange efficiency shows the engine losses due to the

pumping work. Figures 8(c) and 9(c) show the gas exchange efficiencies of methanol- and gasoline-fuelled engines respectively running in HCCI combustion mode at different engine operating conditions. It is observed from Figs 8(c) and 9(c) that the gas exchange efficiency decreases as the mixture becomes leaner for both gasoline and methanol at any inlet air temperature. The maximum gas exchange efficiency for methanol is 96.36 per cent, and for gasoline 93.47 per cent.

4.5 Combustion efficiency

The combustion efficiency is an indicator of how well the engine is burning the fuel. 100 per cent

Fig. 8 Performance parameters for methanol HCCI combustion for different relative air-to-fuel ratios: (a) variation in IMEP; (b) maximum mean gas temperature; (c) gas exchange efficiency; (d) combustion efficiency; (e) indicated thermal efficiency; (f) ISFC

combustion efficiency is not realistically achievable in HCCI; however, a very good combustion efficiency should be around 95 per cent [**23**]. HCCI operation is very sensitive to combustion timing, as it influences the combustion temperature. Late combustion timing means a decreased temperature so that the combustion is inferior and the combustion efficiency is lowered. Figures 8(d) and 9(d) show the combustion efficiencies at different engine operating conditions for methanol and gasoline respectively. The formula for calculation of the combustion efficiency is given in section 2. The maximum combustion efficiency for methanol is found to be 96.6 per cent and for gasoline 91.7 per cent. It can be seen from the figures that the combustion efficiency is lower for gasoline than for methanol at different engine operating conditions.

The combustion efficiency improves as the inlet temperature is raised since the autoignition points are closer and it is easier to achieve more complete combustion.

Figures 8(e) and 9(e) show the gross indicated thermal efficiency for methanol and gasoline respectively at different engine operating conditions in HCCI combustion mode. The formula for calculation of the gross indicated thermal efficiency is given in section 2. These figures show that the indicated thermal efficiency decreases with increasingly leaner mixture. The maximum indicated thermal efficiency achieved is 49 per cent for methanol and 37.95 per cent for gasoline, in HCCI combustion mode.

The indicated specific fuel consumption (ISFC) is the ratio of fuel consumed to the indicated power. The indicated power is calculated from the pressure
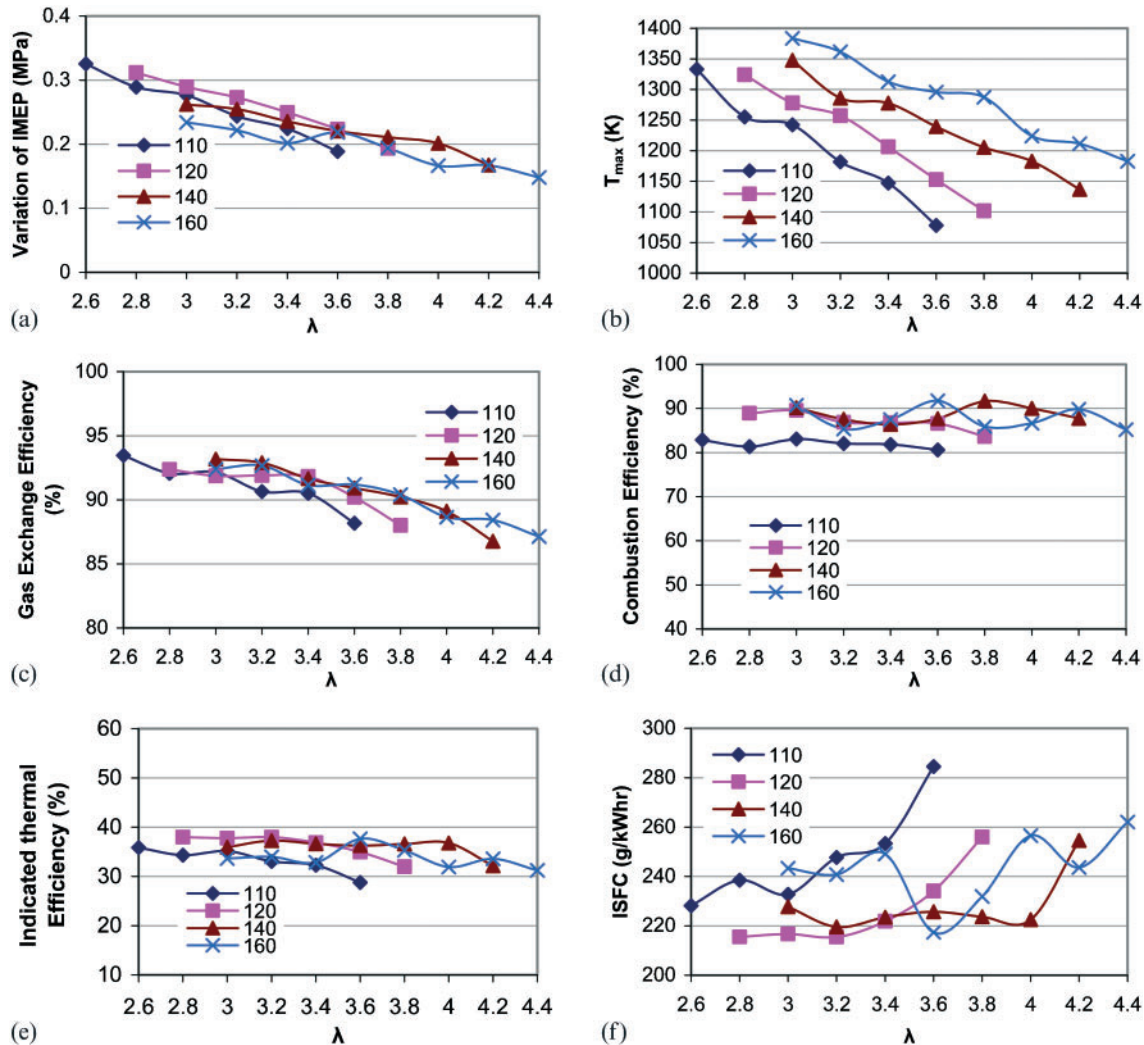
Fig. 9 Performance parameters of gasoline HCCI combustion for different relative air-to-fuel ratios: (a) variation in IMEP; (b) maximum mean gas temperature; (c) gas exchange efficiency; (d) combustion efficiency; (e) indicated thermal efficiency; (f) ISFC

volume curve. Figures 8(f) and 9(f) show the ISFCs for methanol and gasoline respectively at different engine operating conditions in HCCI combustion mode. It can be observed from these figures that the ISFC decreases with increasingly leaner mixtures. This observation is justified since the indicated thermal efficiency has the opposite trend in the HCCI operating region for methanol and gasoline.

5 CONCLUSIONS

The combustion and emission characteristic of a HCCI engine were investigated using a modified two-cylinder engine, in which one cylinder is opera- ted in HCCI combustion mode and the other cyl- inder is operated in conventional diesel mode at a low load for stable engine operations. The inlet air

was supplied in the temperature range 110–160 °C and the engine was operated at a constant engine speed of 1500 r/min, fuelled with methanol or gaso- line. Successful HCCI combustion is obtained in the λ range 3.5–6.5 for methanol and the λ range 2.6–4.4 for gasoline. HCCI mode operation of the engine is within a narrow load range of the engine for both gasoline and methanol. Methanol has a wider operating range than gasoline. The maximum IMEP obtained during the experiment was 3.4 bar for methanol and 3.3 bar for gasoline. The ROHR is high and hence combustion duration is shorter (less than 20° CA) for all the conditions of engine running in HCCI mode using both methanol and gasoline. The gas exchange efficiency is higher for methanol than for gasoline. The combustion efficiency of methanol is also higher than gasoline. The maximum combus- tion efficiency for methanol is 96.6 per cent and for

gasoline 91.7 per cent for the engine operating conditions explored in this investigation. The maximum indicated thermal efficiency was found to be 49 per cent for methanol and 37.95 per cent for gasoline. From these results, it can be concluded that methanol has superior HCCI combustion characteristics compared to gasoline.

© Authors 2009

REFERENCES

1 **Iida, M., Hayashi, M., Foster, D. E.,** and **Martin, J. K.** Characteristics of homogeneous charge compression ignition (HCCI) engine operation for variations in compression ratio, speed, and intake temperature while using n-butane as a fuel. *Trans. ASME, J. Engng Gas Turbines Power*, 2003, **125**, 401–611.

2 Homogeneous charge compression ignition (HCCI) technology. Report to the US Congress US Department of Energy, Energy Efficiency and Renewable Energy, Office of Transportation Technologies, April 2001.

3 **Onishi, S., Jo, S. H., Shoda, K., Jo, D. P.,** and **Kato, S.** Active thermo-atmosphere combustion (ATAC) – a new combustion process for internal combustion engines. SAE paper 790501, 1979.

4 **Ishibashi, Y.** and **Asai, M.** Improving the exhaust emissions of two-stroke engines by applying the activated radical combustion. SAE paper 960742, 1996.

5 **Najt, P. M.** and **Foster, D. E.** Compression-ignited homogeneous charge combustion. SAE paper 830264, 1983.

6 **Thring, R. H.** Homogeneous-charge compression-ignition (HCCI) engine. SAE paper 892068, 1989.

7 **Aoyama, T., Hattori, Y., Mizuta, J.,** and **Sato, Y.** An experimental study on premixed-charge compression ignition gasoline engine. SAE paper 960081, 1996.

8 **Yanagihara, H. A., Satou, Y.,** and **Mizuta, J.** A simultaneous reduction of NO_x and soot in diesel engines under a new combustion system (uniform bulky combustion system UNIBUS). In Proceedings of the 17th International Motor Symposium, Vienna, Austria, 27–28 April 1996, pp. 303–314 (Osterreichischer Verein Fur Kraftfahrzeugtechnik, Vienna).

9 **Yokota, H., Kudo, Y., Nakajima, H., Kakegawa, T.,** and **Susuki, T.** A new concept for low emission diesel combustion. SAE paper 970891, 1997.

10 **Christensen, M., Johansson, B.,** and **Einewall, P.** Homogeneous charge compression ignition (HCCI) using isooctane, ethanol and natural gas – a comparison with spark-ignition operation. SAE paper 972874, 1997.

11 **Christensen, M., Johansson, B., Amnjus, P.,** and **Mauss, F.** Supercharged homogeneous charge compression ignition. SAE paper 980787, 1998.

12 **Walter, B.** and **Gatellier, B.** Near zero NO_x emissions and high fuel efficiency diesel engine: the NADI^{TM} concept using dual mode combustion. *Oil Gas Sci. Technol., Rev. IFP*, 2003, **58**(1), 101–114.

13 **Takeda, Y., Keiichi, N.,** and **Keiichi, N.** Emission characteristics of premixed lean diesel combustion with extremely early staged fuel injection. SAE paper 961163, 1996.

14 **Iwabuchi, Y., Kawai, K., Shoji, T.,** and **Takeda, Y.** Trial of new concept diesel combustion system-premixed compression-ignited combustion. SAE paper 1999-01-0185, 1999.

15 **Kimura, S., Aoki, O., Ogawa, H., Muranaka, S.,** and **Enomoto, Y.** New combustion concept for ultra-clean and high-efficiency small DI diesel engines. SAE paper 1999-01-3681, 1999.

16 **Stanglmaier, R. H.** and **Roberts, C. E.** Homogeneous charge compression ignition (HCCI): benefits, compromises, and future engine applications. SAE paper 1999-01-3682, 1999.

17 **Christensen, M.** and **Johansson, B.** Influence of mixture quality on homogeneous charge compression ignition. SAE paper 982454, 1998.

18 **Christensen, M.** and **Johansson, B.** Homogeneous charge compression ignition with water injection. SAE paper 1999-01-0182, 1999.

19 **Oakley, A., Zhao, H., Ladommatos, N.,** and **Ma, T.** Experimental studies on controlled autoignition (CAI) combustion of gasoline in a 4-stroke engine. SAE paper 2001-01-1030, 2001.

20 **Zhao, F., Asmus, T. W., Assanis, D. N., Dec, J. E., Eng, J. A.,** and **Najt, P. M.** (Eds) *Homogeneous charge compression ignition (HCCI) engines*, 2003 (SAE International, Warrendale, Pennsylvania).

21 **Iida, N.** Combustion analysis of methanol fuelled active thermo-atmosphere combustion (ATAC) engine using spectroscopic observation. SAE paper 940684, 1994.

22 *REVelation operator reference manual*, 2004, pp. 95–96 (Hi-Techniques, Madison).

23 **Muñoz, R. V.** *The performance of a dual fuel HCCI engine*. Master's thesis, Department of Energy Sciences, Lund University, Lund, Sweden, 2006.

24 **Iida, N.** Natural gas HCCI engines. In *CAI and HCCI engines for the automotive industry* (Ed. H. Zhao), 2007 (Woodhead Publishing, Abington, Cambridge).

25 **Christensen, M., Hultqvist, A.,** and **Johansson, B.** Demonstrating the multi fuel capability of a homogeneous charge compression ignition engine with variable compression ratio. SAE paper 1999-01-3679, 1999.

26 **Maurya, R. K.** and **Agarwal, A. K.** Experimental Investigation of cycle-by-cycle variations in CAI/HCCI combustion of gasoline and methanol fuelled engine. SAE paper 2009-01-1345, 2009.

27 **Holman, J. P.** *Experimental methods for engineers,* 6th edition, 1994 (McGraw-Hill, New York).

28 Heywood, J. B. *Internal combustion engine fundamentals*, 1988 (McGraw-Hill, New York).

APPENDIX

Notation

CA	crank angle
CI	compression ignition
COV	coefficient of variation
COV_{IMEP}	coefficient of variation of the indicated mean effective pressure
$dP/d\theta_{max}$	maximum rate of pressure rise
EGR	exhaust gas recirculation
HCCI	homogeneous charge compression ignition
IMEP	indicated mean effective pressure
ISFC	indicated specific fuel consumption
m_f	fuel mass per cycle
q_{LHV}	lower heating value of the fuel
Q_{in}	total heat values of the introduced fuel
ROHR	rate of heat release
SI	spark ignition
SOC	start of combustion
TDC	top dead centre
T_{max}	maximum mean gas temperature
η_{com}	combustion efficiency
η_{ge}	gas exchange efficiency
$\eta_{i,g}$	gross indicated thermal efficiency
λ	relative air-to-fuel ratio